NASA Technical Memorandum 87099

Some Design Philosophy for Reducing the Community Noise of Advanced Counter-Rotation Propellers

James H. Dittmar
Lewis Research Center
Cleveland, Ohio

August 1985

NASA

SOME DESIGN PHILOSOPHY FOR REDUCING THE COMMUNITY NOISE OF ADVANCED

COUNTER-ROTATION PROPELLERS

James H. Dittmar
National Aeronautics and Space Administration
Lewis Research Center
Cleveland, Ohio 44135

SUMMARY

Advanced counter-rotation propellers have been indicated as possibly gen-
erating an unacceptable amount of noise for the people living near an airport.
This report has explored ways to reduce this noise level, which is treated as
being caused by the interaction of the upstream propeller wakes and vortices
with the downstream propeller. The noise reduction techniques fall into two
categories: (1) reducing the strength of the wakes and vortices and (2) reduc-
ing the response of the downstream blades to them. The noise from the wake
interaction was indicated as being reduced by increased propeller spacing and
decreased blade drag coefficient. The vortex-interaction noise could be elim-
inated by having the vortex pass over the tips of the downstream blade, and it
could be reduced by increased spacing or decreased initial circulation. The
downstream blade response could be lessened by increasing the reduced frequency
parameter ω or by phasing of the response from different sections to have
a mutual cancellation effect. Uneven blade to blade spacing for the downstream
blading was indicated as having a possible effect on the annoyance of counter-
rotation propeller noise. Although there are undoubtedly additional methods
of noise reduction not covered in this report, the inclusion of the design
methods discussed would potentially result in a counter-rotation propeller
that is acceptably quiet.

INTRODUCTION

Advanced turboprop aircraft have the potential for significant fuel sav-
ings over equivalent technology turbofan powered aircraft. To investigate this
potential the National Aeronautics and Space Administration has an ongoing
Advanced Turboprop Program (ref. 1). A single rotation turboprop design is
projected to use as much as 15 percent less fuel than turbofans (ref. 1), and
a counter-rotation design may save 8 percent more (ref. 2). Sketches of single
rotation and counter-rotation propellers are shown in figure 1. Recent NASA
propeller research is summarized in reference 3. In order to implement these
fuel savings, however, the new turboprop aircraft must be acceptable to the
public.

The noise of counter-rotation propellers may present a problem for people
living around an airport. Counter-rotation propellers generate more noise
than a single rotation propeller largely because of the flow interaction
between the two propellers. An existing noise model for a propeller in non-
uniform inflow is used herein to represent the interacting noise generated by
counter-rotation propellers. The terms in this noise model are examined in
this report, and methods for reducing the interaction noise are determined.

N86-14007

INTERACTION NOISE MODEL

Formulation

The primary interaction noise mechanism for counter-rotation propellers is represented in figure 2. Trailing behind the forward propeller blades are wakes (fig. 2(a)) and tip vortices (fig. 2(b)). The wakes and vortices strike the downstream propeller blades to create lift fluctuations on the downstream blades, which in turn generate noise. There is, of course, also the interaction of the potential fields of the two propellers, both the front on the rear propeller and the rear on the front propeller. For this discussion the potential field interaction is assumed relatively small compared to wake-vortex interaction with the downstream propeller. However, a number of the methods that will be explored to reduce the wake-vortex interaction noise would also apply to the potential field interaction.

The interaction noise is generated by lift fluctuations on the downstream propeller as the downstream propeller blades pass behind the upstream blades. To model this noise generation, an existing formulation for the loading noise of a propeller operating in a nonuniform inflow will be used. It is assumed herein that the propeller is operating subsonically at takeoff and landing, so that the loading noise is dominant. This formulation is from reference 4 (p. 746), and parts of its derivation are paraphrased for use in explaining the assumptions used in the derivation and in understanding how the noise might be reduced. The derivation presented is not complete, and the reader is directed to reference 4 for further details. Some of the nomenclature has also been changed from reference 4 to avoid confusion with other formulas that will be used later, but the basic derivation has not been altered. More detailed analyses of counter-rotation noise have been performed (for example, see ref. 5), but for the purpose of identifying and understanding the noise reduction possibilities, this simpler model is more easily understood.

The geometry used in this model is for a propeller with B blades rotating at an angular velocity Ω. (See fig. 3.) In this figure r is the distance from the center of the propeller to the location where the noise is measured, θ is the angle measured fore to aft from the propeller axis, and r_1 and φ_1 are the locations of a point on the propeller disk. A complete list of symbols is found in the appendix.

The analysis in reference 4 begins at the case of uniform flow and evaluates the periodic forces on the fluid as two series

$$f_z(t;r_1,\varphi_1) = f_z^0 \sum \alpha_s e^{isB\varphi_1} e^{-is\omega_1 t} \qquad (1)$$

$$f_\varphi(t;r_1,\varphi_1) = f_\varphi^0 \sum \alpha_s e^{isB\varphi_1} e^{-is\omega_1 t} \qquad (2)$$

The constants f_z^0 and f_φ^0 can be expressed in terms of the total thrust force F_t and the total torque T of the propeller as

$$F_t = \int f_z^0 r_1 dr_1 d\varphi_1 \qquad (3)$$

2

$$T = \int (f_\varphi^0 r_1) r_1 \, dr_1 \, d\varphi_1 \tag{4}$$

while the coefficients are obtained from

$$\alpha_s = \frac{1}{f_z^0} \frac{e^{-isB\varphi_1}}{\tau} \int_{-\tau/2}^{\tau/2} f_z(t,\varphi_1) e^{is\omega_1 t} \, dt \tag{5}$$

The analysis proceeds to the nonuniform inflow case by assuming a time independent (although spatially nonuniform) incoming flow field. This would be tne case for a fixed upstream disturbance (like a set of nonrotating upstream vanes), and results in the interaction noise being generated at the blade passage tone of the propeller and its harmonics. The inflow to the downstream propeller of a counter-rotation propeller is not time independent but the assumption is made here since it makes the formulation and result more easily understood. The implications of tne actual rotating incoming distortion will be discussed later. A quasi-steady approach is used to determine the forces resulting from the nonuniform inflow. The nonuniform inflow is assumed small and the widtn of the blade is also assumed sufficiently small so that the thrust and torque respond directly to changes in the velocity. These changes, $v_z(\varphi)$ and $v_\varphi(\varphi)$, would be components of the velocity defect in the wake or vortex from the upstream propeller blade. The constant force amplitudes in equation (1) then become functions of φ_1, as follows:

$$f_z = f_z^0 \left[1 - \frac{2v_\varphi(\varphi)}{V} - \frac{1}{C_t} \frac{dC_t}{d\alpha} \frac{v_z(\varphi)}{V} \right] \equiv f_z^0 \sum_q \beta_q e^{iq\varphi_1} \tag{6}$$

$$f_\varphi = f_\varphi^0 \left[1 - \frac{2v_\varphi(\varphi)}{V} - \frac{1}{C_x} \frac{dC_x}{d\alpha} \frac{v_z(\varphi)}{V} \right] \equiv f_\varphi^0 \sum_q \delta_q e^{iq\varphi_1} \tag{7}$$

where V is the local rotatiɔnal velocity, C_t is the thrust coefficient, C_x is the drag coefficient of the downstream propeller blade, and α is the angle of attack.

From these expressions it is clear that to reduce the forces f_z and f_φ, the velocity defects in the wakes and vortices should be reduced; thus the coefficients β_q and δ_q are also reduced for $q > 0$. The forces on the air are converted into the sound pressure for the propeller by using Green's function. For example, the sound field from the z component of the force is

$$P_z(r,\varphi,\theta) = - \frac{ik_1 \cos\theta}{4\pi r} \sum_{sq} e^{i(sB+q)\theta} e^{isk_1 r} e^{i(sB+q)\varphi - is\omega_1 t}$$

$$\times \int_0^a s f_z^0 \alpha_s \beta_q J_{sB+q}(u) 2\pi r_1 \, dr_1 \, d\varphi_1 \tag{8}$$

3

where

$$u = sk_1 r_1 \sin \theta$$

and

$$K_1 = \frac{\omega_1}{c}$$

Equation 8 sums the contribution from each position on the propeller disk to get the noise at a point in space. As observed through the argument u, the contribution of a given force produces more noise the farther out it occurs on the radius (r_1) of the propeller. This is consistent with the fact that higher velocities near the tip generate more noise. The mean value theorem provides an equivalent radius such that the integrals in equation (8) can be evaluated at that radius. The resultant equation is

$$P = \frac{1}{4\pi r} \sum_{N=1}^{\infty} (2NK_1 \alpha_N) \left\{ \sum_{l=0}^{\infty} \left(\beta_1 F_t \cos \theta + \delta_1 \frac{NB-1}{NBM} F_D \right) \times \right.$$

$$J_{NB-1}(NBM \sin \theta) \times \sin \left[NK_1(r-ct) + (NB-1)(\varphi + \frac{1}{2}\pi) \right. +$$

$$\sum_{l=0} \left(\beta_1 F_t \cos \theta + \delta_1 \frac{NB+1}{NBM} F_D \right) \times J_{NB+1}(NBM \sin \theta) \times$$

$$\left. \sin \left[NK_1(r-ct) + (NB+1)(\varphi + \frac{1}{2}\pi) \right] \right\}$$

(9)

Comparison of Noise Levels and Directivities

The expression for the sound-pressure level at a receiver location (eq. 9) contains the case for a single propeller in uniform flow, obtained by letting l go to 0 and β_0 and $\delta_0 = 1$. The predicted noise from the single rotation propeller in uniform flow is symmetrical and has zeros on the horizontal plane of the propeller axis. Such a propeller has a sharp direc- tivity pattern with no noise on the propeller axis (fig. 4(a)).

The interaction noise from a nonuniform inflow has different directivity. As pointed out in reference 4 for a time-independent nonuniformity, the noise is no longer symmetric. (The effect of the rotating front propeller pattern will be discussed in the section Time Dependent Nonuniformity and Spectra Effects.) The noise also has significant magnitude on the propeller axis. Looking at equation (9) the sound field is composed of two different groups of spinning waves.

$$\omega_- = \frac{NB}{NB-1} \Omega$$

(10)

4

and

$$\omega_+ = \frac{NB}{NB + 1} \Omega \qquad (11)$$

The second wave, which comes from the second l summation, is small because the Bessel functions, of order (NB + 1) greater than one, and argument (NBM sin θ), smaller than order, are small. The first series over l does contain low-order Bessel functions. Some of these Bessel functions have high amplitudes, and as pointed out by reference 4, are larger than the uniform terms (even for small β and δ if the Mach number is less than 1 as it is for the takeoff and landing cases).

This has likely consequences for the cruise noise. At high airplane speeds, such as at cruise, the helical-tip speed of the blades exceeds a Mach number of 1. Here the propeller uniform noise, both loading and thickness, may be dominant, and the interaction noise may not be as important.

Additionally, in the first series over l, some terms have their peak amplitudes on the axis where the single rotation propeller in uniform flow showed no noise. For example the term $l = NB$ contains J_0(NBM sin θ), which has its maximum at $\theta = 0°$ instead of close to $\theta = 90°$. The noise directivity pattern for the nonuniform inflow propeller looks somewhat like figure 4(b) at its peak φ location.

At takeoff and landing conditions the interaction noise, as indicated above, is dominant; thus the noise level of the counter-rotation propeller is raised above the noise level of a single rotation propeller in uniform flow. In addition, and to the disadvantage of the counter-rotation propeller, the directivity pattern would also change. The interaction noise would also increase the area under the airplane that is effected by the noise and increase the time the high noise levels are felt during an airplane flyover. This would significantly increase the Effective Perceived Noise Level (EPNL) and would make the community noise problem even greater.

Time Dependent Nonuniformity and Spectra Effects

As mentioned previously, the noise model of reference 4, equation 9, was developed for time independent nonuniform inflow. The situation for the counter-rotation propeller is, in general, a time-dependent nonuniform inflow to the downstream propeller. This results in the noise being generated at frequencies different than those of the time independent case, but the important parameters that govern the magnitude of the noise remain. Equation (9) can still be used as a model to show what should be done to decrease the magnitude of the interaction noise.

For an understanding of what happens to the frequency of the radiated noise from the counter-rotation propeller, a special case will be investigated first and then a general case will be developed. This discussion is patterned after that of Hubbard (ref. 6). The specific case is a counter-rotation propeller that has the same number of blades in the front propeller as in the rear propeller, with both propellers turning at the same speed. Viewed from a position on a downstream propeller blade, the same upstream propeller blade passes twice in every revolution. With the propellers turning at the same

5

speed, these locations are at two fixed circumferential positions. This is illustrated in figure 5(a) for a counter-rotation propeller which has two blades on each propeller. The front propeller is shaded and the rear propeller is clear. Blade A on the rear propeller encounters (overlaps) blade B of the front propeller at position 2. As the blades continue to rotate, A overlaps B again at position 4 before making a complete revolution. If the two rotational speeds are exactly the same, the positions of the overlaps are fixed.

The noise pattern in the φ direction is also fixed in space and has maxima at the overlap positions and minima in between, as shown in figure 5(b). At a particular spanwise location, the downstream blade experiences what appears to it as time-independent inflow distortions. The magnitude is then adequately represented by equation 9, but the frequency is altered for a fixed observer. The first interaction tone has a frequency that is twice the blade passing frequency (BPF) of each single propeller. In actuality, the first observed interaction frequency is the sum of the BPF's of the individual propellers. This is seen in the double sum over N and 1 in equation (9). A comparison of the spectra from a single rotation propeller and a counter-rotation propeller, with the same number of blades in each row, turning at the same speed, is similar near the minima points in the circumferential directivity where no overlap occurs. However, at the maxima the counter-rotation propeller has extra noise at the harmonics. This is particularly true on the propeller axis where the single rotation propeller theoretically has no noise, but the counter-rotation propeller does have significant noise at twice BPF and beyond.

The overlap and the noise patterns are fixed in space if the two propellers rotate at exactly the same speed. If however, as would generally be the case, the speeds are different and the overlap axes rotate, then, at a fixed observation point, the noise is amplitude modulated. In addition, in a fixed period of time, the downstream blade would experience interactions at the sum of the two blade passing frequencies (BPF). This would also occur if the blade numbers for the two propellers were different. A sample spectra is shown in figure 6. As a result of the double sum in equation (9), all of the cross-interaction frequencies appear. (For example, 3 x BPF_1 plus BPF_2 and BPF_1 plus 3 x BPF_2.) The relative levels of the tones in figure 6 were chosen arbitrarily. The presence of these extra tones in the spectra makes a counter-rotation propeller noisier than a single rotation propeller, particularly at the higher harmonics. Again, the terms impacting the strength's of the interactions are still represented by equation (9) which can be used to identify promising methods of counter-rotation propeller interaction noise reduction.

POSSIBILITIES FOR REDUCING INTERACTION NOISE

The insight into identifying methods to reduce the noise from counter-rotation propellers comes through examining the various terms in equation (9) and the assumptions used in its derivation. Many of the techniques discussed here were first developed for reducing the noise of turbofan engines. For purposes of discussion, the methods seem to fall into the following two categories:

(1) Ways to reduce the wakes and vortices striking the downstream propeller

(2) Ways to reduce the response of the downstream propeller to them

The wake and vortex reductions are discussed with respect to the quasi-steady model of equation (9), and the section Reduced Response discusses the frequency dependent blade response.

Reduced Wakes and Vortices

The forces on the downstream propeller blades are shown in equation (9) in the terms

$$\left(\beta_1 F_t \cos\theta + \delta_1 \frac{NB-1}{NBM} F_D\right)$$

and

$$\left(\beta_1 F_t \cos\theta + \delta_1 \frac{NB+1}{NBM} F_D\right)$$

The general steady thrust and torque on the blade are considered fixed, so that the manner of reducing the interaction forces comes through the coefficients β_1 and δ_1 for $1 > 0$. The expressions for these terms come from equations (6) and (7) where they depend directly on the components of the velocities $v_z(\varphi)$ and $v_\varphi(\varphi)$ that occur in the wakes and vortices of the upstream propeller blades. (See fig. 2.) In order to reduce the interaction noise, the velocity defects from the wakes and vortices that strike the aft propeller need to be reduced. The following will discuss some possible methods to achieve this, treating the wakes and vortices in separate sections.

Wake reduction. - The blades of a propeller act as isolated airfoils near the blade tips and as portions of a cascade near the hub. For this discussion, the wakes are treated as those generated by an isolated airfoil. The maximum velocity defect in the wake of an isolated airfoil has been described in reference 7 as

$$\frac{v}{V_F} = \frac{2.42\sqrt{C_D}}{(X/C_R + 0.3)} \tag{12}$$

where v is the maximum velocity defect in the wake, V_F is the free stream velocity, C_D is the drag coefficient, X is the distance downstream, and C_R is the airfoil chord. The particular velocity diagram for the upstream and downstream propellers determine the components v_z and v_φ of this defect which vary with φ as the downstream blade passes through the wakes. The equation contains two basic terms that can be varied to reduce the wake defect; $\sqrt{C_D}$ and X/C_R. Since the spacing term X/C_R seems to have the most potential for noise reduction it will be discussed first.

Spacing: A possible method of reducing the wake defect velocity, which impacts the downstream propeller and in turn reduces the interaction noise, is

7

to increase the spacing parameter X/C_R, increase the distance x, or reduce the upstream propeller blade chord.

Each hub-to-tip section of the upstream propeller blade has a slightly different wake structure that arrives, because of the different velocity diagrams, at a slightly different time at the downstream propeller blade. The swirl measured behind advanced simple rotation propellers (ref. 3) has been relatively uniform from hub to tip so the arrival times would only be slightly different. For purposes of estimating the effect of spacing, it will be assumed here that all the wakes act in unison and that the sum of all the effects can be approximated by using $20 \log_{10} P$ to calculate the noise. The pressure P is assumed to vary directly with the velocity defect v, so a noise estimation for the effect of spacing can be obtained. The noise reduction with a one chord propeller spacing as the base ($X/C_R = 1$) is shown in figure 7. As can be seen, the noise reduction available from increased spacing is significant. For example, in going from $X/C_R = 1$ to $X/C_R = 2$, the noise is reduced by some 5 dB. Here spacing presents a powerful way to reduce the noise of the counter-rotation propeller. Again, the reduction may not be exactly 5 dB because all of the wakes do not arrive simultaneously. The effect of different response timing can be used to provide some interaction noise reduction and will be discussed later in the section Blade Response.

Reduced drag: The size of the wake defect and in turn the level of interaction noise can be reduced by lowering the drag coefficient of the upstream blades. Using the same $20 \log_{10} P$, as for the spacing estimates, results in the plot of the change in sound pressure with different upstream propeller blade drag coefficients as shown in figure 8.

At first consideration, the ability to reduce the upstream propeller-drag coefficient enough to significantly reduce the noise seems unlikely. However, the blades of the typical advanced turboprop are probably operating in the transonic region near the tip at takeoff or landing condition. As mentioned in the section Interaction Noise Model Formulation, disturbances near the tip generate more noise than inboard. These outboard regions may dominate the noise, and their drag coefficient characteristics will now be discussed.

A typical airfoil type used for the outboard sections of some of the advanced propellers (ref. 3) was the NACA 16 series. The drag coefficient characteristics of this type of airfoil are represented in figure 9 and taken from reference 8. At takeoff or landing, the blades of a counter-rotation propeller would be operating subsonically, probably in the Mach number range from 0.8 to 1.0. As seen in figure 9, this is the drag-rise portion of the blade-operating range and large increases in the drag coefficient exist. If this drag coefficient could be reduced, then a noise reduction could be achieved. For example, if the blade was operating at a drag coefficient of 0.030 and a reduction was achieved to bring that down to 0.010, then the indicated noise reduction from figure 8 would be 5 dB.

At present, there are two methods that could achieve a drag reduction in the Mach number range between 0.8 and 1.0. The first is the use of a different airfoil section that would not exhibit the drag rise in the area of interest, such as the Whitcomb type of airfoil (ref. 9). The second is the use of sweep to lower the relative Mach number on the upstream propeller blade and thereby reduce the drag. In either case, the resultant lower drag coefficient

of the upstream propeller has the potential of significantly reducing the interaction noise. In fact, the use of both supercritical airfoils and sweep should be considered in the propeller design.

The use of sweep on single rotation propellers has been shown to reduce the uniform flow noise also. Figure 10 shows a plot from reference 10 where three single rotation propellers exhibited different noise characteristics with sweep. The SR-2 blade was straight, while the SR-1M blade had 30° of tip sweep. The sweep here was done for aerodynamic purposes and resulted in a delay of the noise rise to a higher helical tip Mach number. The SR-3 blade had 45° of tip sweep and was designed to have the sweep acoustically tailored for noise reduction. The additional amount of sweep here has delayed the rise to an even higher Mach number, and the tailoring of the sweep has resulted in a lower asymptotic level. This tailoring of the sweep will be discussed later in the section Reduced Response, as to its use on the downstream propeller blades to reduce the blade response.

In general, it appears that sweep should specifically be designed into the leading propeller because it has the potential for reducing both the noise of the upstream propeller and the interaction noise of the counter-rotation propeller combination. Forward sweep on the front propeller might also be considered since it increases the spacing between the two propellers.

Vortex reduction. - The upstream propeller blade tips trail behind them vortices which, when interacting with the downstream propeller, are potentially a larger interaction noise generator than the propeller wakes. Pressure measurements on the pressure side of a simulated wing surface installed behind a single rotation advanced propeller are shown in figure 11 which was taken from reference 11. Here, it can be seen that the fluctuations in the vortex region are larger than those for the inboard wake positions. When this is combined with the noise generation mechanism (eq. (9)), that produces more noise for disturbances at the tip than those inboard, the importance of the vortex-propeller interaction becomes clear.

In addition to an axial velocity defect the vortex brings about the fluctuating lift on the downstream blade by the speed at which it rotates about the core, its rotational velocity. It is primarily this circulation velocity, when broken down into v_z and v_φ, that produces the noise. A model for a viscous vortex was presented in reference 12 based on the work of reference 13. A model of the maximum circulation velocity was found in reference 14 to be

$$v_{\theta_{max}} = \frac{C_v r_o}{(X/C_R)^{1/2}}$$

(13)

The possibilities for reducing vortex-propeller interaction noise are discussed in the following paragraphs.

Avoidance: Although it might just as easily be discussed in the section Response Reduction, the avoidance of the vortex is discussed first since the design of the upstream blade may be a factor. Obviously, if the tip vortex does not strike the downstream blades, it will not be an interaction noise source. It is, of course, not possible to avoid the upstream propeller wake,

9

but since the vortex is so localized near the tip it may be possible to have it pass over the downstream propeller blade tip.

It may be possible to design the nacelle such that enough radially outward velocity remains to sweep the vortex outwardly over the downstream blades. If this is not possible, the downstream blades might be shortened slightly so that they miss the vortices. Hopefully this could be done without too great a loss in performance. In any case, design consideration should be directed toward having the downstream propeller miss the upstream vortex since this would result in a significant noise reduction.

Spacing: As seen in equation (13) the strength of the vortex does reduce with spacing. The decay is not as strong as it is for a wake, which is consistent with a vortex being more persistent than a wake. Using the same $20 \log_{10} P$, as for the wake noise model, results in the vortex noise decay with spacing and is shown in figure 12. As seen, for example, in going from $X/C_R = 1$ to $X/C_R = 2$, the noise reduction is approx. 3 dB. This is only about one-half of the amount obtained for the wake decay.

Reduction of Circulation: A reduction in the initial vortex circulation would reduce the interaction noise also. Here the circulation velocity goes directly as the initial circulation, and, by using the same $20 \log_{10} P$, the noise would be reduced 6 dB for every halving of the initial circulation. The initial vortex circulation might be reduced by a different blade design, or the spanwise flows that create the tip vortex might be blocked by placing small fences along the upstream blade at different positions. In reference 15, fences were successfully used to reduce the losses and vortices near the wall of a turbine stage for turbofan engines. The fences would, of course, create vortices themselves, which would be smaller than the tip vortex, and being more inboard would create less noise. In any case, the reduction of the initial vortex circulation could result in a significant reduction in this interaction noise source.

Reduced Response

The wakes and vortices from the upstream propeller strike the downstream blades and create fluctuating forces that produce noise. The previous sections of this report have concentrated on reducing the magnitude of the wakes and vortices as a means of noise reduction. The following sections will discuss ways to reduce the fluctuating forces that result from a given wake or vortex.

Reduction of Fluctuating Lift. - In the derivation of equation (9), the nonuniform inflow was assumed to be relatively small and the width of the downstream blade chord was sufficiently small such that the thrust and torque responded directly to the changes (defects, etc.) in the incoming velocity; that is, a quasi-steady response. In reality, the downstream blades would have chords large enough so that they would not respond in this manner. A better expression for the response involves the ratio of the blade chord to the incoming velocity wave length. An example of this type of response dependence can be found in reference 16 for an isolated flat plate with a gust input transverse to the chord. The fluctuating lift pressure is indicated as

10

$$\Delta L_N = 2\pi\rho U \sin \bar{\beta} \ \Psi e^{i\nu t} S(\omega) \tag{14}$$

The fluctuating lift is still linearly dependent on the wake defect (Ψ, the gust variation), so the previous discussions of wake and vortex reductions still apply. However, the proportionality of the response is no longer one to one, but is modified by the Sear's function $S(\omega)$. A plot of $S(\omega)$ is shown in figure 13. As seen, if the downstream blade chord is sufficiently small, ω approaches zero and $S(\omega)$ has a real component of 1. In other words, it responds in a quasi-steady manner as indicated in the initial assumptions that led to equations (6) and (7). However, as the chord of the downstream blade becomes larger, ω increases and the response magnitude and phase both change. In other words, the response is no longer in phase and it has less magnitude. As ω increases the function spirals inward toward zero. A plot of the reduced magnitude with increasing ω is shown in figure 14.

As seen by increasing ω from 0.4 to 0.8 (a doubling) the magnitude of the lift response, and thereby the noise, would be reduced approx. 4 dB. This increase in ω could be brought about by an increase in the chord of the downstream blade or by a decrease in the incoming gust wavelength L. The incoming gust wavelength is given by the incoming velocity divided by a product of the upstream blade number and the rotational speed of the pattern relative to the downstream blade

$$L = \frac{U_I}{B_u(\Omega_u + \Omega_D)} \tag{15}$$

So L could be increased by increasing the number of blades in the upstream propeller B_u, or by increasing the rotational speeds of the propellers ($\Omega_u + \Omega_D$). The increasing of the rotational speeds would produce higher uniform-flow noise (source alone with no interaction) and would probably not be advantageous from that standpoint. The increasing of the number of upstream blades would be feasible and should therefore be considered.

The response of an actual airfoil to gusts in both longitudinal as well as transverse directions is of course different than the flat-plate analysis presented here. An analysis of this type can be found in reference 17. However, the general concept of reduced response with an increase in the reduced-frequency parameter is still valid. In summary, increased upstream blade number and increased downstream propeller chords are desired design features to reduce counter-rotation propeller noise at takeoff and landing conditions.

Phasing. - In the previous wake-spacing section, the noise was estimated by using $20 \log_{10} P$ and by assuming that all hub-to-tip sections were acting in unison. In actuality the wakes from the upstream propeller may not strike the downstream blade in unison. In general, the section wakes travel at slightly different speeds and at different angles. They might arrive somewhat along a line as shown in figure 15(a). This results in the section wakes interacting with the downstream blades at slightly different times. Since they are not all striking at once, the response of the downstream blade is somewhat less. This phasing of the wake interactions can be tailored to provide a noise reduction feature. This is done by providing some cancellation of the lift fluctuations from one section by that of another.

11

A similar method was applied to the stator of a fan stage in reference 18 with the technique outline in reference 19. The design considered both skewing the blades to the wake front (in-plane sweep), as shown in figure 15(b), and axial sweep, as in figure 15(c), to achieve the desired phasing. The final design of reference 15 only needed the sweep to accomplish its goal, so the skewing of the blades was not used. The application of this phasing technique to the downstream propeller could be done similarly to the stator design.

Similar phasing was used for uniform-flow propeller noise in the design of the SR-3 propeller (ref. 20). This technique swept the blades such that the noise from the different blade sections, acting in a phase relationship, provided some mutual cancellation. As seen in figure 10, this phasing from the tailored sweep brought about some 6 dB of noise reductions at the design condition (asymptotic level). The same phasing could be applied, by using sweep or skew, to the interaction noise generated on the downstream counter-rotation propeller. Since sweep has already reduced propeller noise (no distortion), it would probably be the preferred method of achieving the phasing. The amount of reduction achieved by sweep on a single rotation propeller indicates that phasing should be considered as a design technique to reduce the community noise of counter-rotation propellers.

Frequency Modification. - It may be advantageous, from an annoyance standpoint, to modify the amount of noise occurring in particular harmonics even if the total noise is not changed. One method of doing this is to stagger the blades of a propeller so that the spacing between blades is not equal (ref. 21). This may, of course, create some balance problems for a propeller design. However, if a particular harmonic was indicated as controlling the perceived noise of the propeller, this technique might be used to shift some of the noise to other harmonics and reduce the annoyance.

CONCLUDING REMARKS

Since an advanced counter-rotation propeller may create an unacceptable amount of noise for the people living near an airport, this report has explored ways to reduce this noise level. The interaction of the two propellers was judged to be the source that caused the counter-rotation propeller to be noisier than an equivalent single rotating propeller. Specifically, the interaction of the upstream propeller wakes and vortices with the downstream propeller was considered to be the dominant mechanism. A number of techniques were explored to reduce the strength of these interactions. They fell generally into the following two groups:

(1) Those that reduced the wakes and vortices acting on the downstream propeller

(2) Those that reduced the response of the downstream blades to those velocities

The techniques studied and their potential noise reductions were the following:

(1) Reduced wakes and vortices

(a) Reduced wakes

12

(1) Increased spacing to chord ratio – An increase in spacing
from $X/C_R = 1$ to $X/C_R = 2$ indicates a 5 dB reduction.

(2) Decreased upstream blade drag coefficient – A reduction in
drag coefficient from 0.030 to 0.010 indicates a 5 dB
reduction.

(b) Reduced vortex

(1) Avoidance – Having the vortices pass over the downstream
blades would eliminate this noise source.

(2) Increased spacing to chord ratio – An increase in spacing
from $X/C_R = 1$ to $X/C_R = 2$ indicates a 3 dB reduction.

(3) Reduced initial vortex circulation – Cutting the initial
circulation in half would indicate a 6 dB reduction.

(2) Reduced Response

(a) Reduction of fluctuating lift – An increase in the reduced
frequency parameter ω from 0.4 to 0.8 would indicate a 4 dB
reduction.

(b) Phasing of the blade section responses to provide mutual
cancellation – When this technique was applied to the uniform
flow noise of a single rotation propeller a noise reduction of
6 dB was observed.

(c) Frequency Modification by uneven blade spacing of the downstream
propeller blades – Although the overall noise would probably not
go down with this technique, the change in frequency content
could reduce the annoyance.

The noise reductions from these techniques would not directly add together if
incorporated in a propeller, and these are undoubtedly not the only ways to
reduce the interaction noise. However, the inclusion of the design methods
discussed would potentially result in a counter-rotation propeller that is
acceptably quiet.

REFERENCE

1. Whitlow, J.B., Jr.,; and Sievers, G.K.: Fuel Savings Potential of the
NASA Advanced Turboprop Program. NASA TM-83736, 1984.

2. Strack, W.C.; et al.: Technology and Benefits of Aircraft Counter Rota-
tion Propellers. NASA TM-82983, 1982.

3. Mikkelson, D.C.; Mitchell, G.A.; and Bober, L.J.: Summary of Recent NASA
Propeller Research. NASA TM-83733, 1984.

4. Morse, P.M.; and Ingard, K.U.: Theoretical Acoustics. McGraw-Hill, 1968,
pp. 737-747.

5. Hanson, D.B.: Noise of Counter Rotation Propellers, AIAA Paper 84-2305, Oct. 1984.

6. Hubbard, H.H.: Sound from Dual-Rotating and Multiple Single-Rotating Propellers. NACA TN-1654, 1948.

7. Silverstein, A.; Katzoff, S.; and Bullivant, W.K.: Downwash and Wake Behind Plain and Flapped Airfoils. NACA Rep. 651, 1939.

8. Propeller Performance Analysis, Aerodynamic Characteristics. NACA 16 Series Airfoils, Part II, C-2000, Curtis Wright Co, Aug. 1949.

9. Whitcomb, R.T.: Review of NASA Supercritical Airfoils. ICAS Paper 74-10, Aug. 1974.

10. Dittmar, J.H.; Jeracki, R.J.; and Blaha, B.J.: Tone Noise of Three Supersonic Helical Tip Speed Propellers in a Wind Tunnel. NASA TM-79167, 1979.

11. Miller, B.A.; Dittmar, J.H.; and Jeracki, R.J.: The Propeller Tip Vortex - A Possible Contributor to Aircraft Cabin Noise. J. Aircr., vol. 19, no. 1, Jan. 1982, pp. 84-86.

12. Dosanjh, D.S.; Gasparek, E.P.; and Eskinazi, S.: Decay of a Viscous Trailing Vortex. Aeronautical Quarterly, vol. 13, May 1962, pp. 167-188.

13. Newman, B.G.: Flow in a Viscous Trailing Vortex. Aeronautical Quarterly, vol. 10, May 1959, pp. 149-162.

14. Dittmar, J.H.: Interaction of Rotor Tip Flow Irregularities with Stator Vanes as a Noise Source. AIAA Paper 77-1342, Oct. 1977.

15. Rohlik, H.E.; et al.: Secondary Flows and Boundary-Layer Accumulations in Turbine Nozzles NACA Rep. 1168, 1954.

16. Sears, W.R.: Some Aspects of Non-Stationary Airfoil Theory and Its Practical Application. J. Aeronaut. Sci., vol. 8, no. 3, Jan. 1941, pp. 104-108.

17. Goldstein, M.E.; and Atassi, H.: A Complete Second-Order Theory for the Unsteady Flow About an Airfoil Due to a Periodic Gust. J. Fluid Mech., vol. 74, pt. 4, Apr. 22, 1976, pp. 741-765.

18. Hayden, R.E.; et al.: Analysis and Design of a High Speed, Low Noise Aircraft Fan Incorporating Swept Leading Edge Rotor and Stator Blades. (BBN-3332, Bolt Beranek and Newman; NASA Contract NAS3-18512.) NASA CR-135092, 1977.

19. Bliss, D.B.; Chandiramani, K.L.; and Piersol, A.G.: Data Analysis and Noise Prediction for the QF-1B Experimental Fan Stage. (BBN-3338, Bolt Beranek and Newman; NASA Contract NAS3-19426). NASA CR-135066, 1976.

20. Rohrbach, C.; et al.: Evaluation of Wind Tunnel Performance Testings of an Advanced 45° Swept Eight-Bladed Propeller at Mach Numbers from 0.45 to 0.85, NASA CR-3505, 1982.

21. Mellin, R.C.; and Sovran, G.: Controlling the Tonal Characteristics of the Aerodynamic Noise Generated by Fan Rotors. J. Basic Eng., vol. 92, no. 1, Mar. 1970, pp. 143-1254.

Symbol List

a_m equivalent radial location, length

B number of blades in propeller

B_u number of blades in upstream propeller

C_D drag coefficient

C_p blade chord (downstream propeller), length

C_R airfoil chord, length

C_t thrust coefficient

C_v fixed value for a given airfoil (eq. (13)), 1/length

C_x drag coefficient (eq. (7))

c speed of sound, length/time

F_D drag force of propeller, force

F_t thrust of propeller, force

f_z periodic fluid force in z direction (eq. (1)), force

f_z^0 force constant (eq. (3)), force

f_φ periodic fluid force in φ direction (eq. (2)), force

f_φ^0 force constant (eq. (4)), force

i $\sqrt{-1}$

$J_D(E)$ Bessel function of order D, argument E

K_1 $= \omega_1/C$

L incoming gust wavelength, length

m $= a_m\Omega/C$ = rotational Mach number at equivalent radial location, a_m

P sound pressure at receiver, force/length^2

P_z sound pressure from z component of force

r distance to noise measurement location (fig. 3), length

r_1 radius to a location on the propeller disk (fig. 3), length

$S(\omega)$ Sear's response function

16

s	summation index, (eq. (8))
T	torque of propeller, length-force
t	time
U	incoming freestream velocity to airfoil, length/time
U_I	incoming velocity (eq. (15))
u	$sk_1 r_1 \sin \theta$
V	blade local rotational velocity, length/time
V_F	freestream velocity (eq. (12)), length/time
v	maximum velocity defect in wake, length/time
$v_z(\varphi)$ and	
$v_\varphi(\varphi)$	components of velocity defect in z and φ directions, length/time
$v_{\theta_{max}}$	maximum circulation velocity in vortex, length/time
x	coordinate axis (fig. 3), length
x	distance downstream of airfoil, length
z	axial distance along propeller axis (fig. 3), length
α	angle of attack, radians
α_s	Fourier coefficient (eq. (5))
β	absolute flow angle at entrance to propeller blade, radians
β_q	distortion coefficient (eq. (6))
Γ_0	initial vortex circulation, $(length)^2/time$
ΔL_N	fluctuating lift pressure, force/area
δ_q	distortion coefficient (eq. (7))
θ	angle fore to aft from propeller disk (fig. 3), radians
ν	frequency of gust, radians/time
ρ	fluid density, mass/length^3
φ	angle in circumferential direction (fig. 3), radians
φ_1	angular location of point on propeller disk (fig. 3), radians

Ψ magnitude of gust variation, length/time

Ω angular velocity of propeller (fig. 3), radians/time

Ω_D angular velocity of downstream propeller, radians/time

Ω_u angular velocity of upstream propeller, radians/time

ω reduced frequency parameter = $\pi C_p/L$, radians

ω_1 blade passing frequency = $B\Omega$, radians/time
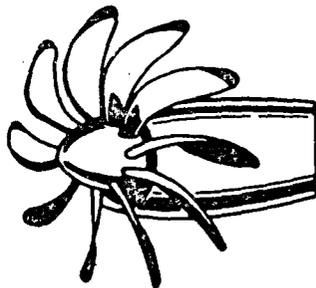
(a) Single rotation.
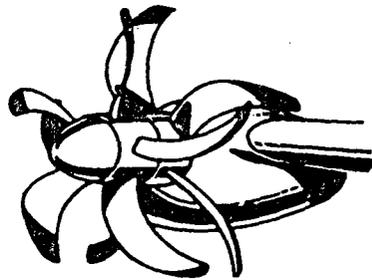
(b) Counter rotation.

Figure 1.- Advanced propellers.

Upstream propeller

Propeller wake

Wake interacts with
downstream propeller

Downstream
propeller

(a) Wake interaction.

Upstream propeller

Propeller tip vortex

Vortex interacts with
downstream propeller

Downstream
propeller
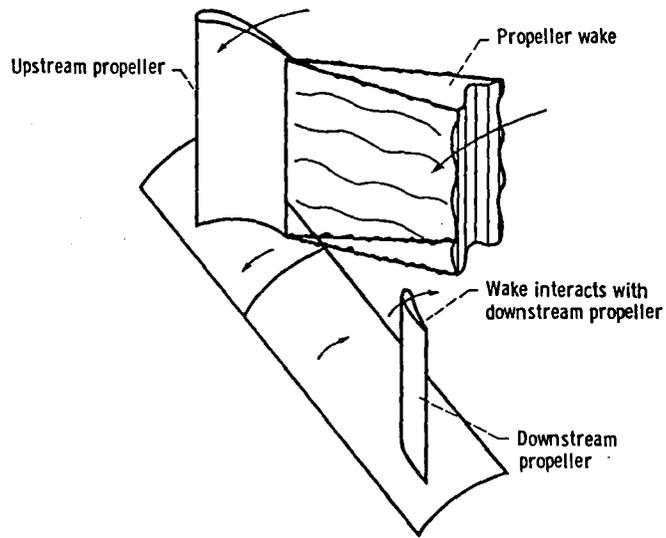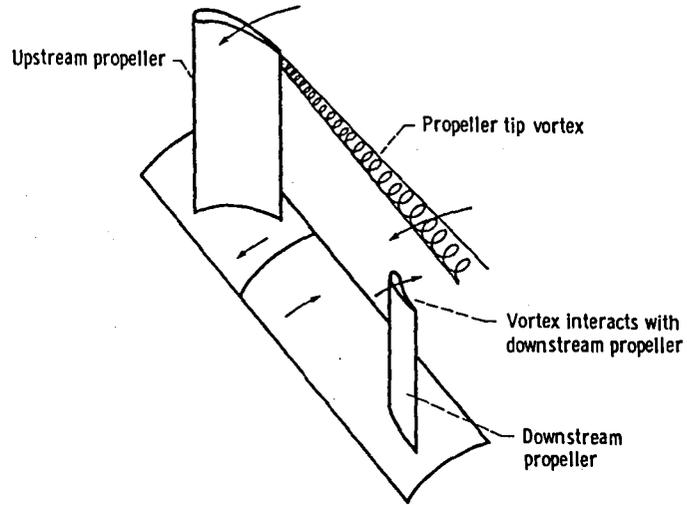
(b) Vortex interaction.

Figure 2. - Noise mechanisms.
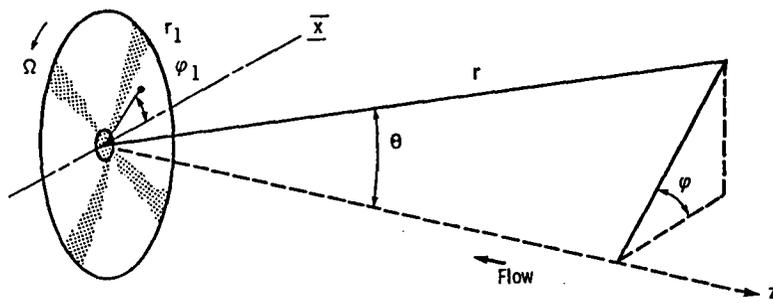
Figure 3.- Propeller coordinates (ref. 4).
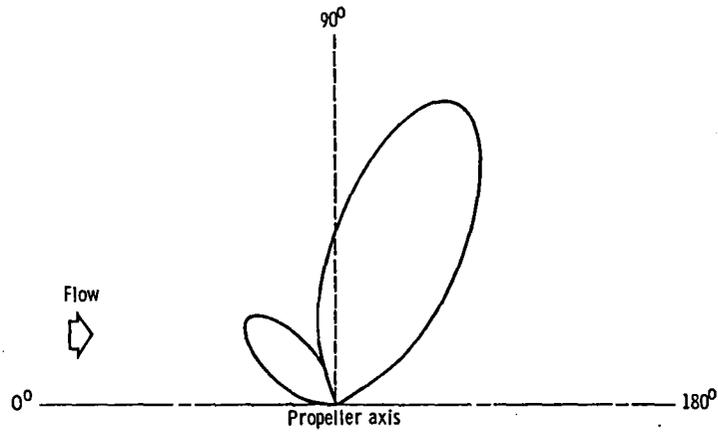
(a) Noise pattern with uniform flow (circumferential symmetric directivity).

Figure 4.- Blade passage tone directivity.
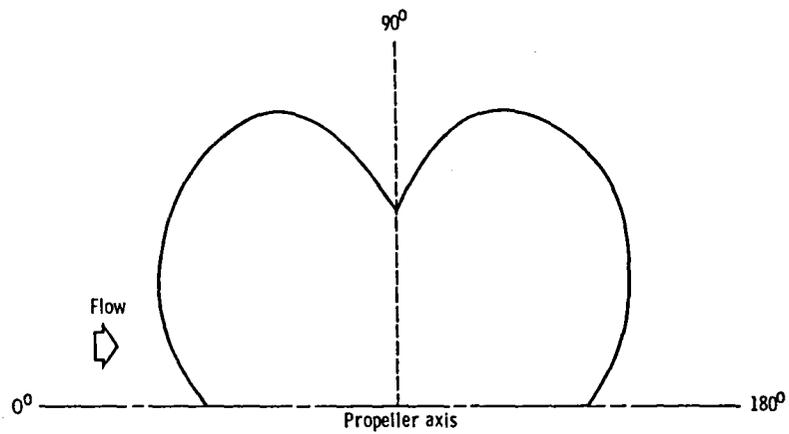
(b) Possible noise pattern with nonuniform inflow at the circumferential angle of the peak noise.

Figure 4.- Concluded.
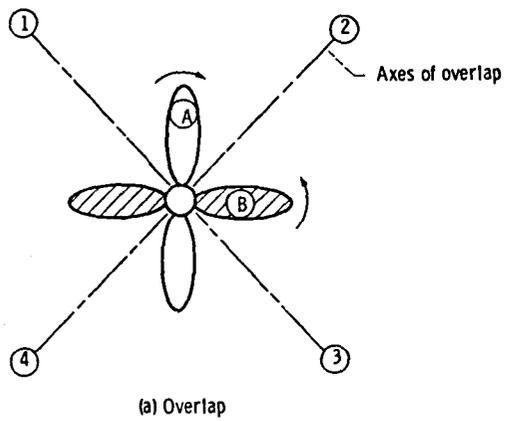
(a) Overlap
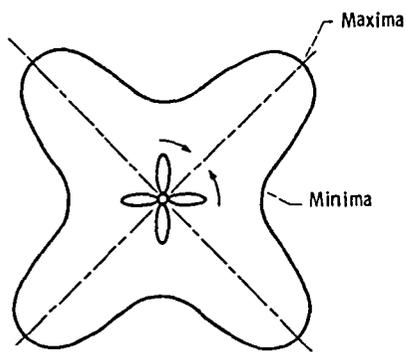
(b) Noise pattern

Figure 5. - Counter-rotating propeller overlap.
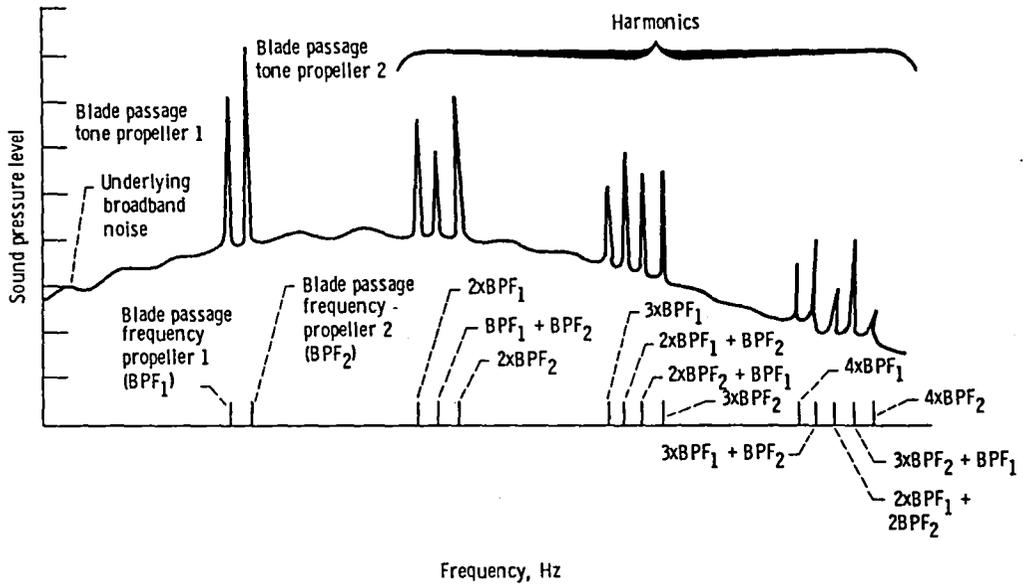
Figure 6.- General counter-rotating propeller noise spectra.
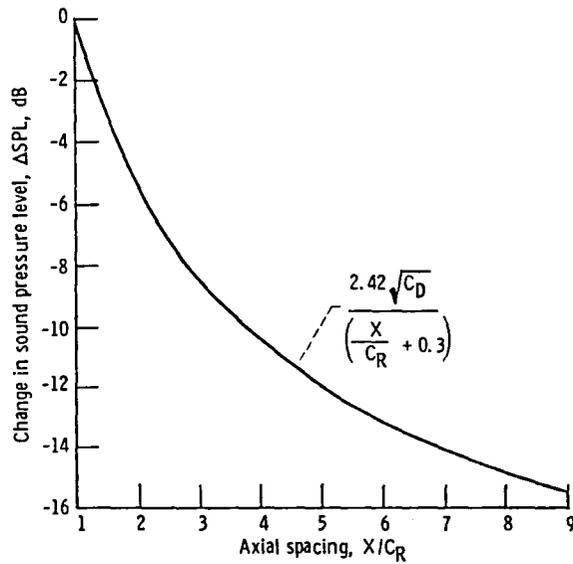
Figure 7.- Change in sound pressure level with spacing for wake.
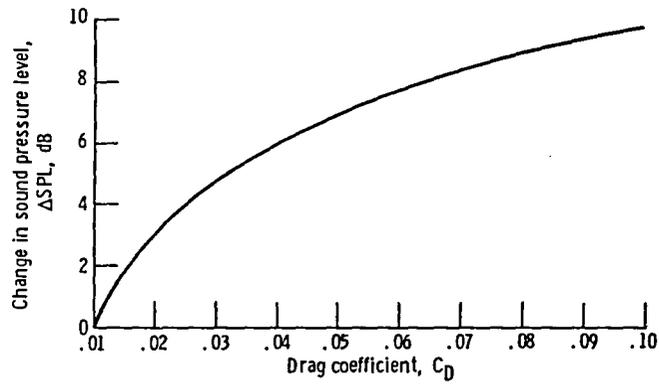
Figure 8.- Change in sound pressure level with upstream propeller
drag coefficient.
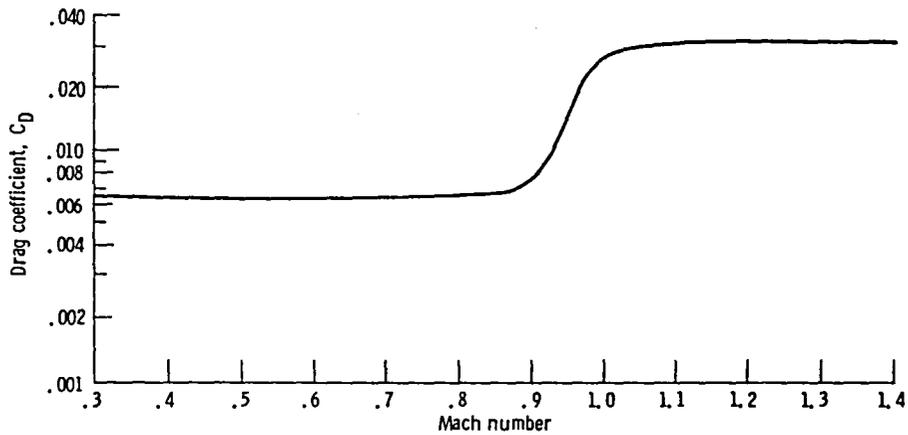
Drag coefficient versus Mach number; lift coefficient, 0.2

Figure 9. - Airfoil performance characteristics. Airfoil section NACA 16-004; aspect ratio, ∞
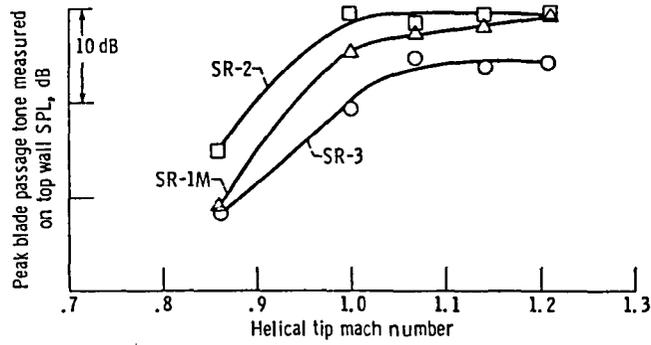
Figure 10. - Maximum blade passage tone variation with helical tip Mach number (ref. 10). (All at nominal advance ratio of 3.06.)
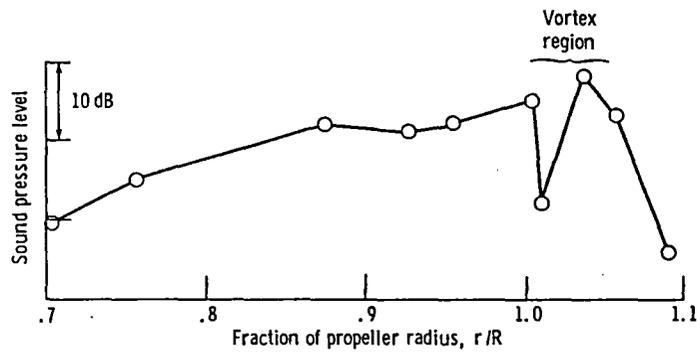
Figure 11. - Radial variation of vane surface sound pressure level at propeller blade passing frequency (ref. 11); $M_0 = 0.8$, $J = 3.06$, $C_p = 1.66$, $M_t = 1.15$.
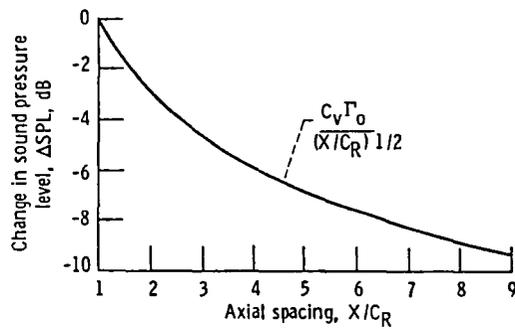
Figure 12. - Change in sound pressure level with spacing for vortex (ref. 14).
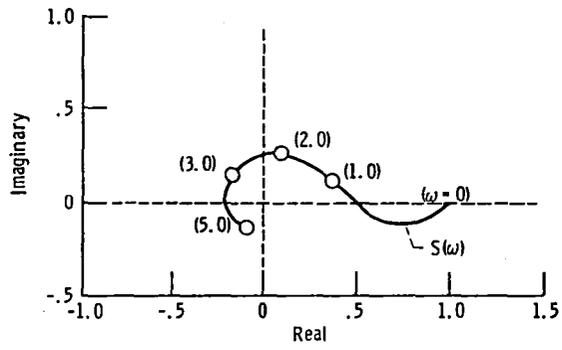
Figure 13.- Variation of response function with reduced frequency parameter, ω.
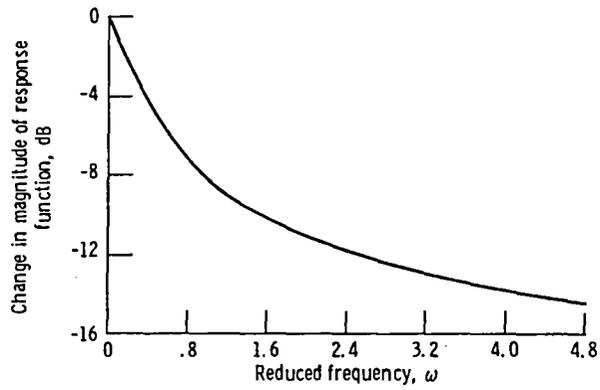

Figure 14.- Change in magnitude of response function with reduced frequency parameter, ω.
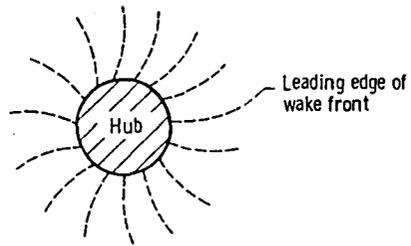
(a) Nonradial wake front.
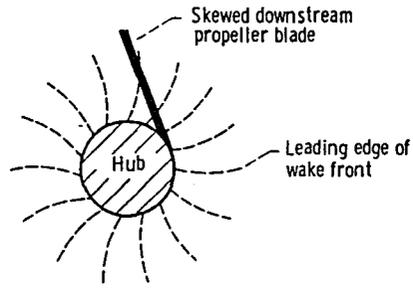
(b) Skewed downstream blades.
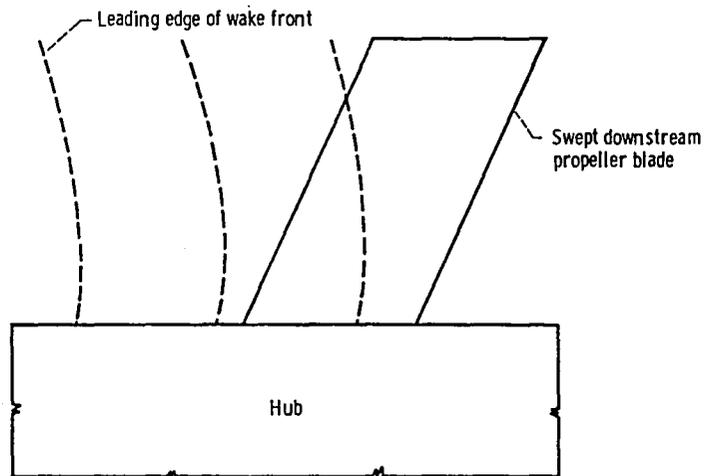
(c) Swept downstream blades.

Figure 15. - Phasing.

1. Report No. NASA TM-87099	2. Government Accession No.	3. Recipient's Catalog No.
4. Title and Subtitle Some Design Philosophy for Reducing the Community Noise of Advanced Counter-Rotation Propellers		5. Report Date August 1985
		6. Performing Organization Code 505-45-58
7. Author(s) James H. Dittmar		8. Performing Organization Report No. E-2692
		10. Work Unit No.
9. Performing Organization Name and Address National Aeronautics and Space Administration Lewis Research Center Cleveland, Ohio 44135		11. Contract or Grant No.
		13. Type of Report and Period Covered Technical Memorandum
12. Sponsoring Agency Name and Address National Aeronautics and Space Administration Washington, D.C. 20546		
		14. Sponsoring Agency Code

15. Supplementary Notes

16. Abstract

Advanced counter-rotation propellers have been indicated as possibly generating an unacceptable amount of noise for the people living near an airport. This report has explored ways to reduce this noise level, which is treated as being caused by the interaction of the upstream propeller wakes and vortices with the downstream propeller. The noise reduction techniques fall into two categories: (1) reducing the strength of the wakes and vortices and (2) reducing the response of the downstream blades to them. The noise from the wake interaction was indicated as being reduced by increased propeller spacing and decreased blade drag coefficient. The vortex-interaction noise could be eliminated by having the vortex pass over the tips of the downstream blade, and it could be reduced by increased spacing or decreased initial circulation. The downstream blade response could be lessened by increasing the reduced frequency parameter ω or by phasing of the response from different sections to have a mutual cancellation effect. Uneven blade to blade spacing for the downstream blading was indicated as having a possible effect on the annoyance of counter-rotation propeller noise. Although there are undoubtedly additional methods of noise reduction not covered in this report, the inclusion of the design methods discussed would potentially result in a counter-rotation propeller that is acceptably quiet.

17. Key Words (Suggested by Author(s)) Propeller noise; Noise; Counter-rotating propeller	18. Distribution Statement Unclassified - unlimited STAR Category 71

19. Security Classif. (of this report) Unclassified	20. Security Classif. (of this page) Unclassified	21. No. of pages	22. Price*

End of Document